Composites Part B 176 (2019) 107333

Contents lists available at ScienceDirect

Composites Part B

journal homepage: www.elsevier.com/locate/compositesb

Free vibration characteristics of glass and bamboo epoxy laminates under hygrothermal effect: A comparative approach

Moumita Sit, Chaitali Ray *

Department of Civil Engineering, Indian Institute of Engineering Science and Technology, Shibpur, Howrah, 711103, India

ARTICLE INFO

Keywords:
A. Laminates
B. Environmental degradation
B. Vibration
C. Finite element analysis (FEA)

ABSTRACT

The present paper attempts to identify the suitability of natural fibre composite as a potential substitute of conventional synthetic fibre reinforced composite materials. Experimental and numerical models are developed to study the variation of vibration characteristics and other engineering properties of both types of laminates in hygrothermal environment. A finite element model based on Green–Lagrange type nonlinear third order shear deformation theory is developed to account for the nonlinear behaviour induced due to hygrothermal effect. A computer code is developed using MATLAB. The laminates are prepared in the laboratory by adopting vacuum bagging technique. The present numerical model is validated by comparing the solutions with experimental results. A comparative study in the perspective of hygrothermal effects on dynamic characteristics of glass fibre reinforced polymer (GFRP) composites and bamboo mat reinforced polymer (BMRP) composites is carried out. The study reveals that the vibration characteristics of BMRP laminates are comparable to glass fibre reinforced plastic (GFRP) laminates even in elevated temperature and moisture.

1. Introduction

Synthetic fibres such as glass, carbon and aramid are being used in numerous applications ranging from aerospace components to civil infrastructures for several years. However, high cost of production and material of some fibres including their adverse effects on the environment have led to renewed interest towards the development of eco-friendly, recyclable or sustainable materials. As a result, increasing interest in utilising less expensive natural fibres instead of synthetic fibres as reinforcement in composites has taken place. Although natural fibre reinforced polymer matrix composites possess innumerable beneficial properties like low density, abundant availability and biodegradability, they are highly sensitive to environmental influences such as temperature rise and water absorption. Because of its structure and composition, natural fibre absorbs moisture when it is exposed to humid conditions or immersed in water. The mechanical properties of natural fibres may be altered to a considerable extent due to moisture absorption depending on the varieties of fibres.

Although slightly inferior to fibreglass in terms of mechanical properties, bamboo fibres are approximately 10 times cheaper than fibreglass [1]. Numerous studies were carried out to utilize locally available and physically or chemically treated bamboo as reinforcement for composites [2–9] in recent past. Li et al. [10] investigated the performance of laminated bamboo columns under axial compression. Several researchers [11,12] developed polypropylene based bamboo composites and evaluated the mechanical properties of such composites. Investigations were also carried out for bio based polymer composites consisting of natural fibres and biodegradable resin [13–16]. Only a few investigations are reported on the study of bamboo fibre reinforced composites using thermosetting matrix such as epoxy and polyeseter resin [17–21]. However, very limited literature is available on the investigation of layered composite laminates made of bamboo [22–24]. Stiffness and mechanical properties (tensile, compression, flexural strength and screw holding capabality) of laminated bamboo composites were evaluated by the researchers [22–24]. The majority of the available literature focus on the mechanical properties of the bamboo based composites, whereas only very few literature is available which address the effect of environmental factors considering elevated temperature or moisture absorption on the mechanical properties of bamboo fibre composites [25–29]. In a review by Zakikhani et al. [30], bamboo fibre materials have been compared with the glass fibre in terms of their mechanical property, recyclability and environment sustainability.

The extensive literature review reveals that the free vibration analysis of bamboo based bio composites is not studied till date. Moreover,

* Corresponding author.
E-mail addresses: moumita.sit11@gmail.com (M. Sit), chaitali@civil.iiests.ac.in (C. Ray).

https://doi.org/10.1016/j.compositesb.2019.107333
Received 3 January 2019; Received in revised form 6 July 2019; Accepted 11 August 2019
Available online 12 August 2019

all the previous research works were carried out to determine the mechanical properties of bamboo reinforced composites. Determination of the engineering properties including Modulus of elasticity (E), Modulus of rigidity (G) and Poisson's ratio (ν) of bamboo epoxy composites is also not reported so far in the published literature. The comparative study of bamboo and glass epoxy laminates in hygrothermal conditions is also scarce in available literature. To the best of authors' knowledge, no previous study is available in the existing literature on the material degradation of BMRP and GFRP laminates with temperature change/moisture absorption experimentally. However it is necessary to identify the pattern of material degradation of both BMRP and GFRP to predict the actual behaviour of laminates in the hygrothermal environment which may be useful for future research and practical application.

The material degradation due to change in temperature or moisture absorption is an essential aspect which influences the mechanical behaviour of laminated composites considerably. Due to the thermal expansion of polymer matrix, volume change of composite laminates occurs. The volume change during moisture absorption is caused by swelling of matrix and is considered analogous to thermal expansion. As a result, the geometry of structure or a structural component gets distorted and loses stable configuration. This in turn induces initial strain leading to significant geometric nonlinearity. Thus, assessment of the dynamic characteristics of laminated composite requires the consideration of initial stains due to the effect of temperature change/moisture absorption.

The present paper aims to conduct a comparative study on the dynamic behaviour of hygrothermally affected GFRP and BMRP composite laminates. Nonlinear terms including large deflection and large rotation using Green Lagrange strains are taken into account to develop the present finite element model based on the third order shear deformation theory (TSDT). Experimental investigations on the free vibration of glass fibre reinforced polymer (GFRP) and locally available untreated bamboo mat reinforced polymer (BMRP) laminates at different temperature levels and moisture concentrations are also conducted. The laminates have been prepared in the laboratory and the material properties are measured with reference to ASTM standard. The consistency between the experimental mode shapes and numerical mode shapes is verified by using CrossMAC (modal assurance criterion) in the present study. The results will be a guideline for the acceptance of bamboo fibre as a suitable alternative reinforcing material instead of glass fibre.

2. Numerical analysis

The temperature distribution across the thickness of the laminate is obtained from the solution of a steady-state 1D Fourier heat conduction equation

$$\frac{d}{dz}\left(kA\frac{dT}{dz}\right)+S=0 \tag{1}$$

where, k, A, T and S are thermal conductivity, cross sectional area perpendicular to the heat flow direction, specified temperature rise and rate of heat generation per unit volume respectively. The moisture diffusion in the laminate with time is obtained from Fick's second law of diffusion

$$\frac{\partial C}{\partial t}=D\frac{\partial^2 C}{\partial x^2} \tag{2}$$

where, x the is the distance in the thickness direction, C is the moisture concentration and D is the coefficient of constant diffusion. The initial strain of a lamina developed due to temperature change and moisture absorption is expressed as

$$\begin{bmatrix} e_x \\ e_y \\ e_s \end{bmatrix}_k = \begin{bmatrix} \alpha_x \\ \alpha_y \\ \alpha_s \end{bmatrix}_k \Delta T + \begin{bmatrix} \beta_x \\ \beta_y \\ \beta_s \end{bmatrix}_k \Delta C \tag{3}$$

α_x, α_y, and α_s are the coefficients of thermal expansion and β_x, β_y and β_s are the coefficients of moisture expansion. The deviation of temperature from ambient temperature (20 °C) is ΔT and ΔC is the percentage of moisture absorption. The stress resultants induced by hygrothermal effect are expressed as

$$\mathbf{N}_i^{HT}, \mathbf{M}_i^{HT} = \sum_{k=1}^{n}\int_{z_{k-1}}^{z_k}\left(\overline{\mathbf{Q}_{ij}}\right)_k\{e_i\}(1,z)dz; i, \quad j=x,y,s \tag{4}$$

where, $\mathbf{N}_i^{HT}$ and $\mathbf{M}_i^{HT}$ are the membrane and bending stress resultants respectively and $(\overline{\mathbf{Q}_{ij}})_k$ is the transformed reduced elastic stiffness matrix.

2.1. Finite element formulation

The plate element is modelled by using eight noded isoparametric quadratic plate bending element having seven degrees of freedom (DOF) per node, viz., u, v, w, θ_x, θ_y, ζ_x, ζ_y for the present analysis. Third order shear deformation theory with Green-Lagrange nonlinear approach for laminated plate is applied in the present formulation. The characteristic equation for the static analysis of a structural system can be written in the matrix form as

$$\mathbf{K\delta}=\mathbf{P} \tag{5}$$

where $\mathbf{P}$ is the thermal load vector. The constitutive equation for laminated plate under thermal load is presented as

$$\mathbf{F^{HT}}=\mathbf{D\varepsilon}-\mathbf{F} \tag{6}$$

where $\mathbf{F}$ is the stress resultant vector of the laminated plate and s is the hygrothermal stress resultant vector. The stress resultants are written as

$$\mathbf{F}=\left\{N_x \quad N_y \quad N_{xy} \quad M_x \quad M_y \quad M_{xy} \quad P_x \quad P_y \quad P_{xy} \quad Q_x \quad Q_y \quad R_x \quad R_y\right\}^T \tag{7}$$

$$\mathbf{F^{HT}}=\left\{N_x^T \quad N_y^T \quad N_s^T \quad M_x^T \quad M_y^T \quad M_s^T \quad P_x^T \quad P_y^T \quad P_s^T \quad 0 \quad 0 \quad 0 \quad 0\right\}^T \tag{8}$$

Dis the rigidity matrix of the laminated plates and the elements of**D**matrix are defined as

$$\left(\mathbf{A}_{ij},\mathbf{B}_{ij},\mathbf{C}_{ij},\mathbf{E}_{ij},\mathbf{F}_{ij},\mathbf{H}_{ij}\right)=\sum_{k=1}^{n}\int_{z_{k-1}}^{z_k}\left(\overline{\mathbf{Q}_{ij}}\right)_k\left(1,z,z^2,z^3,z^4,z^6\right)dz, i, \quad j=x,y,s \tag{9}$$

$$\left(\mathbf{A}_{ij}^z,\mathbf{B}_{ij}^z,\mathbf{C}_{ij}^z\right)=\sum_{k=1}^{n}\int_{z_{k-1}}^{z_k}\left(\overline{\mathbf{Q}_{ij}}\right)_k\left(1,z^2,z^4\right)dzi, \quad j=x,y,s \tag{10}$$

The stiffness matrix for the plate element is given by

$$\mathbf{K}_e=\int_A \mathbf{B}^T\mathbf{D}\mathbf{B}dA \tag{11}$$

where, $\mathbf{B}$ is the strain-displacement matrix and defined by the derivative of shape functions. The elements of $\mathbf{B}$ matrix are described in Sit et al. [31].

2.1.1. Nonlinearity due to hygrothermal effect

The present geometric nonlinear model is developed by considering the Green–Lagrange strain displacement relation. The composite plate tends to undergo geometric distortion due to temperature rise and/or moisture absorption causing hygrothermal stress that alters the free vibration frequencies significantly. The nonlinear strain components in the vector form, can be represented as

$$\boldsymbol{\varepsilon}_{NL}=\left\{\varepsilon_{xnl}\varepsilon_{ynl}\gamma_{xynl}\gamma_{xznl}\gamma_{yznl}\right\}^T \tag{12}$$

The nonlinear strain components are defined in Eq. (A.1). The elemental initial stress stiffness matrix $\mathbf{K}_{\sigma e}$ for geometric distortion due to hygrothermal load can be expressed as

$$\mathbf{K}_{\sigma e} = \iint \mathbf{B}_{NL}^{T} \mathbf{L} \mathbf{B}_{NL} dxdy \tag{13}$$

where, $\mathbf{B}_{NL}$ is the matrix relating non-linear strain-displacement. The elements of $\mathbf{B}_{NL}$ matrix are given in Eq. (A.2). The elements of $\mathbf{L}$ matrix are specified in Eq. (A.3).

2.1.2. Element mass matrix

The consistent mass matrix based on the displacement field using TSDT of the plate element is formulated and expressed by

$$\mathbf{M}_e = \int_{-1}^{1} \int_{-1}^{1} \mathbf{S}^T \mathbf{m}_k \mathbf{S} |\mathbf{J}| \, d\xi \, d\eta \tag{14}$$

The shape function matrix $\mathbf{S}$ and the mass component matrix $\mathbf{m}$ are derived according to Biswas and Ray [32].

2.1.3. Element load vector

The element load vector $\mathbf{P}_{\mathbf{e}}^{\mathbf{HT}}$ due to the temperature change/moisture absorption is calculated as

$$\mathbf{P}_{\mathbf{e}}^{\mathbf{HT}} = \int_{-1}^{1} \int_{-1}^{1} \mathbf{B}^T \mathbf{F}^{\mathbf{HT}} |\mathbf{J}| \, d\xi \, d\eta \tag{15}$$

2.2. Solution process

The final equation can be solved by using the Eigen value method and the stepwise procedure is presented as following:

- Elemental stiffness matrix, mass matrix and initial stress stiffness matrix are developed using the FEM solution. Initial stress stiffness matrix is calculated by considering the effect of hygrothermal load.
- The global stiffness and mass matrices are calculated by assembling the elemental matrices.
- The natural frequencies are determined from the following dynamic equilibrium equation,

$$\mathbf{K} + \mathbf{K}_{\sigma e} - \omega_n^2 \mathbf{M} = 0 \tag{16}$$

3. Experimental procedures

3.1. Materials

Epoxy resin ARALDITE® CY 230-1 IN is used as matrix for the present study. ARADUR® HY 951 IN is used as hardener for curing in 10:1 ratio. For BMRP composites, the middle section of a matured *Bambusa balcooa* bamboo plant is used in this investigation. The density distribution of fibres in the bamboo plant varies according to the radial position in the cross section and along the length of the plant. The fibre density is much higher in the outer skin region than in the inner region [33]. Experimental results [33] indicate that stiffness and strength under tensile loading of bamboo laminae is higher in outer region and lower in inner region. Therefore, all the sticks used in this investigation were from middle region to minimize variability in material properties. The bamboo section was split into round sticks in machine. The sticks used for laminates are 1.35–1.40 mm thick (radial direction in the plant) and approximately 300 mm long. Bi-directional E-glass fabric has been used for the present investigation for GFRP composites. Thickness of the glass fabric is 1 mm.

3.2. Fabrication of composite laminates

Resin infusion process is adopted to fabricate the laminates using vacuum bagging technique. The air inside the bag is extracted by a vacuum pump (−100 kPa) and thus atmospheric pressure can be applied to the laminate to consolidate it while maintaining ambient temperature (20 °C). BMRP and GFRP composite laminates, prepared in the laboratory, are shown in Fig. 1(a)–(b) respectively.

3.3. Testing

3.3.1. Nondestructive testing

Nondestructive testing (NDT) is applied to determine the engineering properties (Modulus of elasticity (E), Modulus of rigidity (G) and Poisson's ratio (ν)) of the laminates. The NDT approach is carried out using Olympus 45 MG ultrasonic thickness gage as well as longitudinal and shear wave transducers. The transducers along with appropriate instrumental set up measure longitudinal and shear wave sound velocities of the test specimens. The velocities thus obtained are incorporated into the equations available in the ASTM -E494-10, Standard Practice for Measuring Ultrasonic Velocity in Materials [34].

3.3.2. Testing for moisture absorption and temperature rise

The fabricated BMRP and GFRP specimens are tested for temperature rise and moisture absorption. Dimensions of each specimen are 250 mm × 250 mm. Bamboo-epoxy laminates consist of 4 layers and have average thickness of 5.5 mm. Glass-epoxy laminates consist of 5 layers and have average thickness of 5 mm. Since the bamboo mat and the glass fabric are having different thickness, bamboo-epoxy and glass epoxy laminates prepared in the laboratory also have different thickness. The temperature variation was maintained between 20 °C to 120 °C and the plates were kept in heat chamber for 24 h to achieve desired temperature rise. For moisture absorption, one set of plate specimen were kept immersed in saline water and another in tap water. The percentage of moisture absorption (ΔC) at different time intervals is determined by the following equation

$$\Delta C = \frac{\left(w_t - w_{dry}\right)}{w_{dry}} \times 100$$

where, w_t is the weight of wet specimen at specific time interval and w_{dry} is the weight of dry specimen.

3.3.3. Experimental modal analysis

The experimental modal analysis is carried out to determine the natural frequencies of the composite laminates at different level of temperature elevation and moisture concentration. Five specimens are used for each investigation and the average value is obtained. The experimental modal analysis is performed by using the accelerometer (B & K type-4507), an impact hammer (B & K type-8206) and B & K Photon plus data acquisition system in the present investigation. The impact applied by the impact hammer is received by the accelerometer which is positioned at a selected node of the plate. The input and output data stored in the photon plus data acquisition system are analysed by using FFT based RT pro software for the modal analysis. The entire set up of the present experimental procedure is shown in Fig. 2. The frequency response functions (FRFs) of the plate are measured by the RT pro signal analysis application. The natural frequencies are determined from the measured FRFs. The post processing of acquired data using the pulse reflex software has been carried out to determine the mode shapes obtained experimentally.

4. Results and discussion

4.1. Convergence study

A convergence study is conducted for the hygrothermal free vibration analysis of composite laminates to verify the consistency of the proposed finite element model and to identify the optimum mesh division of the proposed FE model. The convergence study is performed on

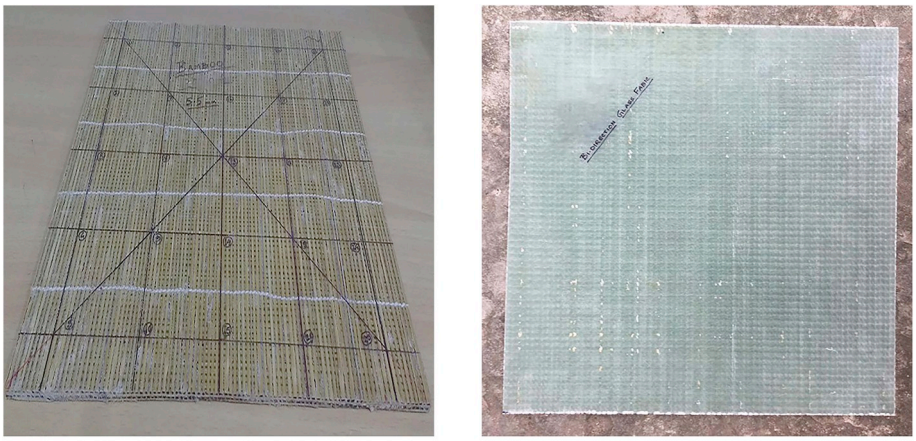

(a) (b)

Fig. 1. (a) BMRP laminate; (b) GFRP laminate.

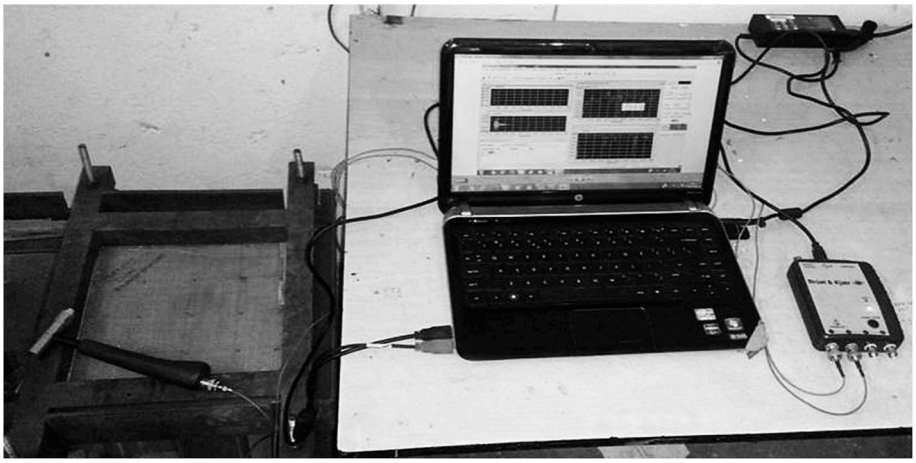

Fig. 2. Experimental set up for modal analysis.

the nondimensional fundamental frequencies of symmetric (0°/90°/90°/0°) four layered cross-ply graphite epoxy composite laminated plate and presented in Table 1 considering the following parameters:

a/b = 1, a/t = 100, $E_1 = 130$ GPa, $E_2 = 9.5$ GPa, $G_{12} = G_{13} = 6.0$ GPa, $G_{23} = 0.5G_{12}$, $\nu_{12} = 0.3$, $\alpha_1 = -0.3 \times 10^{-6}$/K, $\alpha_2 = 28.1 \times 10^{-6}$/K, $\beta_1 = 0$, $\beta_2 = 0.44$, $\Delta T = 25$K, $\Delta C = 0.1\%$.

It is observed from Table 1, that the nondimensional frequencies of composite plates under hygrothermal effect converge reasonably well with mesh refinement. It is also observed that 10×10 mesh division is adequate to predict the higher order nonlinear behaviour accurately and applied for the present numerical analysis.

Table 1
Convergence study of nondimensional fundamental frequencies for all edges simply supported laminated composite plate under hygrothermal effect.

Mesh size	$\Delta C = 0.1\%$			$\Delta T = 25$ K		
	Mode 1	Mode 2	Mode 3	Mode 1	Mode 2	Mode 3
4×4	9.01	19.485	38.916	7.812	18.152	38.094
8×8	9.308	19.979	39.110	8.019	18.619	38.861
10×10	9.33	19.983	39.114	8.021	18.623	38.865
12×12	9.33	19.983	39.114	8.021	18.623	38.865

4.2. Characterization of composite laminates

4.2.1. Moisture absorption profile

The plates were kept immersed in saline water and in tap water separately and moisture absorption of the laminates was measured at a time interval of 10 days for a total period of 365 days. The water uptake of the BMRP laminate is compared to that of the GFRP laminate. The moisture absorption curve as a function of immersion time is presented in Fig. 3. The trend seems to follow the Fickian type diffusion. It is noted that BMRP laminate absorbs more moisture than that of GFRP laminate for same period of immersion. It is also observed that the percentage of moisture uptake is higher for tap water than that of saline water due to higher density of saline water as an obvious reason. The untreated BMRP laminate immersed in tap water reaches maximum saturation level at a faster rate and remains almost constant thereafter. Finally the difference of maximum moisture absorption is not very high. The maximum amount of water uptake in GFRP and BMRP laminates are 1.75% and 1.9% respectively.

4.2.2. Determination of material properties of the laminates at different levels of temperature and moisture concentration

The measured longitudinal (V_L) and transverse (V_T) sound velocities at x, y and z directions in BMRP and GFRP laminates (at ambient temperature and dry condition) are presented below:

BMRP: $V_L^x = V_L^y = 3626$m/sec; $V_L^z = 2256$m/sec; $V_T^x = V_T^y = 1872$m/sec; $V_T^z = 1256$m/sec

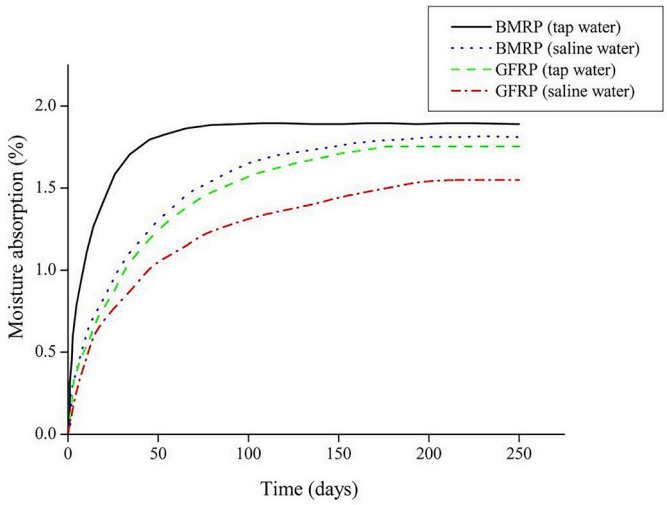

Fig. 3. Moisture absorption curve of GFRP and BMRP laminates.

GFRP: $V_L^x = V_L^y = 4457$m/sec; $V_L^z = 2399$m/sec; $V_T^x = V_T^y = 2378$m/sec; $V_T^z = 1390$m/sec

The material properties of the laminates are computed as per ASTM E494-10 for different levels of temperature increment and moisture absorption. The material properties of the dry specimens at ambient temperature are obtained as follows:

BMRP: $E_1 = E_2 = 20.9$ GPa, $G_{12} = 2.89$ GPa, $G_{23} = G_{13} = 8.41$ GPa, $\nu_{12} = 0.275$, $\nu_{23} = \nu_{13} = 0.318$, $\rho = 1830$ kg/m^3

GFRP: $E_1 = E_2 = 30.4$ GPa, $G_{12} = 3.99$ GPa, $G_{23} = G_{13} = 11.7$ GPa, $\nu_{12} = 0.247$, $\nu_{23} = \nu_{13} = 0.301$, $\rho = 2064$ kg/m^3

The degradation of material properties with temperature increment is shown in Fig. 4(a) which depicts that the material properties E_1 (or E_2) and G_{12} of both types of laminates decrease. For 100 °C temperature rise, the percentage reduction in Modulus of elasticity are around 40.65% and 43.61% respectively for GFRP and untreated BMRP laminates whereas the Modulus of rigidity degrades up to 30.02% and 31.07% respectively.

The degradation of material properties due to moisture absorption are shown in Fig. 4(b). For maximum percentage of moisture absorption the reductions in Modulus of elasticity (E_1) are around 62% and 72.48% respectively for GFRP and BMRP laminates. The percentage reduction in Modulus of rigidity (G_{12}) ranges up to 47.79% and 61.92% respectively.

As the laminates are fully immersed with exposed boundaries, most severe moisture absorption occurs and the maximum possible degradation is observed from Fig. 4(a)–(b).

4.3. Modal analysis of laminates subjected to hygrothermal effect

New results based on the nonlinear TSDT model are presented and verified experimentally as no result is available in the published literature on the vibration characterization of GFRP and BMRP laminates under hygrothermal effect.

4.3.1. Modal analysis of laminates for temperature increment

Laboratory made GFRP and BMRP laminates (5 nos. of each type) of dimensions 250 mm × 250 mm have been considered for the present analysis. The average thickness of GFRP and BMRP plates are obtained as 5 mm and 5.5 mm respectively. The plates are kept in heat chamber at desired temperature rise. Various boundary conditions (Fig. 5(a) and Fig. 5(b)) are considered including simply supported (SSSS), clamped (CCCC) and free-free.

The results in terms of modal frequencies of laminates obtained from the present nonlinear FE model based on TSDT and the experimental investigation are compared. The natural frequencies obtained for free-free boundary condition for both GFRP and BMRP laminates are presented in Table 2. It is observed from Table 2 that the natural frequencies decrease with increase in temperature for both GFRP and BMRP laminates in case of free-free boundary condition. It is also noted that the natural frequencies obtained from experimental and numerical investigations are in excellent agreement, percentage deviation remaining less than 5%. Table 2 also shows that the difference between the natural frequencies of GFRP and BMRP laminates with temperature rise remains within 6%. The difference between the natural frequencies of GFRP and BMRP laminates does not vary significantly with temperature increment. This is because of the polymer matrix is mainly affected due to temperature rise whereas the reinforcement fibres remain unaffected.

The sample mode shapes obtained from experiment as well as the present FE model corresponding to the first three modal frequencies of GFRP laminates with free-free support condition for 100 °C temperature rise are shown in Fig. 6. The mode shapes obtained from experiments and numerical modelling show very good resemblance with each other. The correlation between the experimental and numerical mode shapes is indicated by using CrossMAC (modal assurance criterion). The value of MAC ranges from 0 to 1 which specifies the degree of correlation between the mode shapes. The CrossMAC matrix for the mode shapes are shown in Table 3. The diagonal terms denote the consistency between

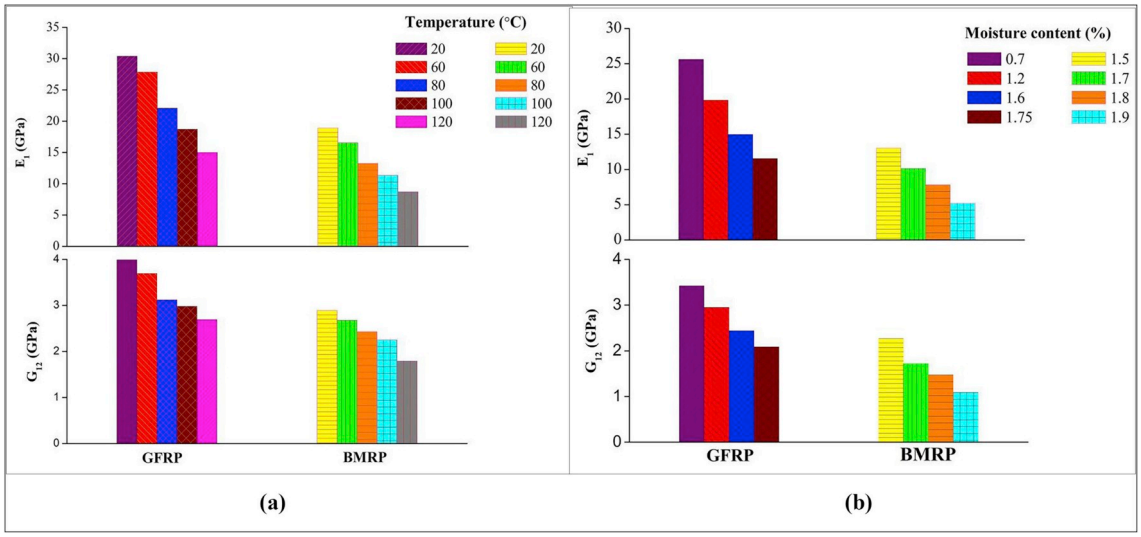

Fig. 4. Degradation of material properties with (a) temperature rise; (b) moisture absorption.

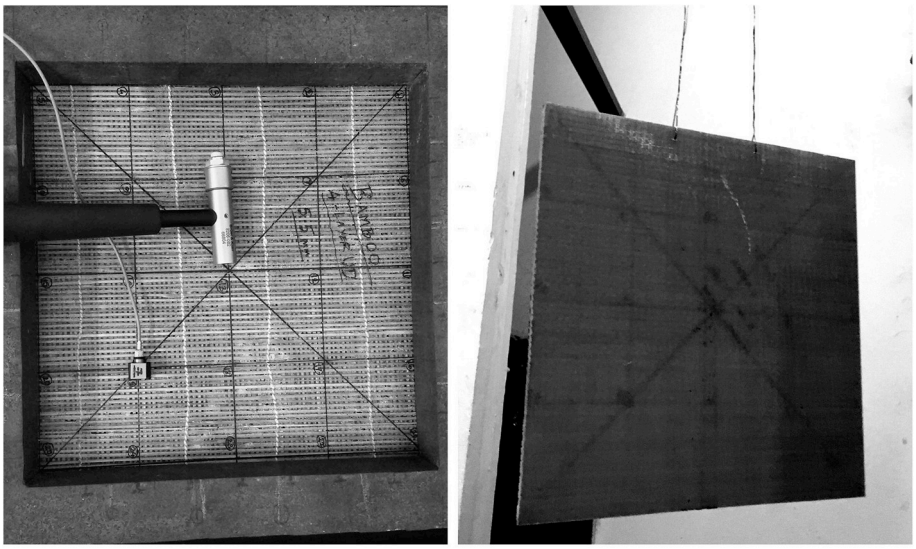

Fig. 5. Setup for (a) simply supported and clamped boundary conditions; (b) free-free boundary condition.

Table 2
Natural frequencies for free-free GFRP and BMRP laminates at different temperature levels.

T (°C)	Type of laminate	Natural frequencies (Hz)						Deviation (%)		
		FEM			Experimental			(Experimental-FEM)/Experimental		
		Mode 1	Mode 2	Mode 3	Mode 1	Mode 2	Mode 3	Mode 1	Mode 2	Mode 3
20	GFRP	190.51	525.08	761.71	194.53	535.53	779.69	2.07	1.95	2.31
	BMRP	181.74	500.84	725.72	186.85	515.77	747.93	2.73	2.89	2.97
Difference (%) (GFRP-BMRP)		4.60	4.62	4.73	3.95	3.69	4.07	–	–	–
60	GFRP	182.64	503.50	730.22	186.93	516.04	750.72	2.29	2.43	2.73
	BMRP	171.56	473.32	684.91	176.73	487.47	706.28	2.93	2.90	3.03
Difference (%) (GFRP-BMRP)		6.06	5.99	6.20	5.46	5.54	5.92	–	–	–
80	GFRP	165.79	457.27	663.37	169.43	467.28	680.55	2.15	2.14	2.52
	BMRP	157.51	432.05	626.17	161.78	444.88	644.89	2.64	2.88	2.90
Difference (%) (GFRP-BMRP)		5.00	5.51	5.61	4.52	4.79	5.24	–	–	–
100	GFRP	156.40	431.53	625.80	159.59	440.07	639.19	2.00	1.94	2.09
	BMRP	148.01	407.71	591.13	151.71	417.73	607.22	2.44	2.40	2.65
Difference (%) (GFRP-BMRP)		5.37	5.52	5.54	4.94	5.08	5.00	–	–	–
120	GFRP	145.91	403.09	583.91	148.77	411.51	600.37	1.92	2.05	2.74
	BMRP	137.52	379.29	550.14	141.02	389.11	566.42	2.48	2.52	2.87
Difference (%) (GFRP-BMRP)		5.75	5.90	5.78	5.21	5.44	5.65	–	–	–

mode shapes obtained from experimental model and the present FE model. The CrossMAC matrix is defined in Eq. (B.1) in Appendix B.

The numerical values of MAC in the diagonal cells are marked bold and are varying from 0.9 to 0.94 which indicate excellent correlation and consistency between the mode shapes obtained numerically and experimentally as shown in Fig. 6.

The fundamental frequencies obtained for simply supported as well as clamped boundary conditions are presented in Fig. 7.

It is observed from Fig. 7 that same trend of reduction of frequency is followed for both GFRP and BMRP. The fundamental frequencies get reduced with the increase in temperature for simply supported and clamped boundary condition. Change in temperature induces initial stresses in the structures which causes reduction in stiffness of the structure. The stiffness of the composite plate tends to reduce with the increment in temperature, and thus reduces the corresponding frequency. However the slope of reduction curve remains identical irrespective of boundary condition. The fundamental frequencies of GFRP and BMRP laminates reduce by 31.01% and 33.23% respectively for 100 °C rise of temperature. The rate of reduction in frequencies is marginally higher for BMRP laminates. It is also noted that the natural frequencies are found to be lowest for free-free boundary condition and highest in case of clamped boundary condition for both GFRP and BMRP laminates, as expected.

4.3.2. Modal analysis of laminates for moisture absorption

The GFRP (5 mm thick) and BMRP (5.5 mm thick) laminates are kept immersed in both tap water and saline water. It is observed that the amount of water uptake is higher in case of tap water (section 4.2.1) for both GFRP and BMRP laminates. The percentage of moisture concentration (ΔC) is measured at different time intervals. The rate of moisture absorption of GFRP and BMRP laminates are different. Therefore, the amount of water uptake varies for GFRP and BMRP laminates at any

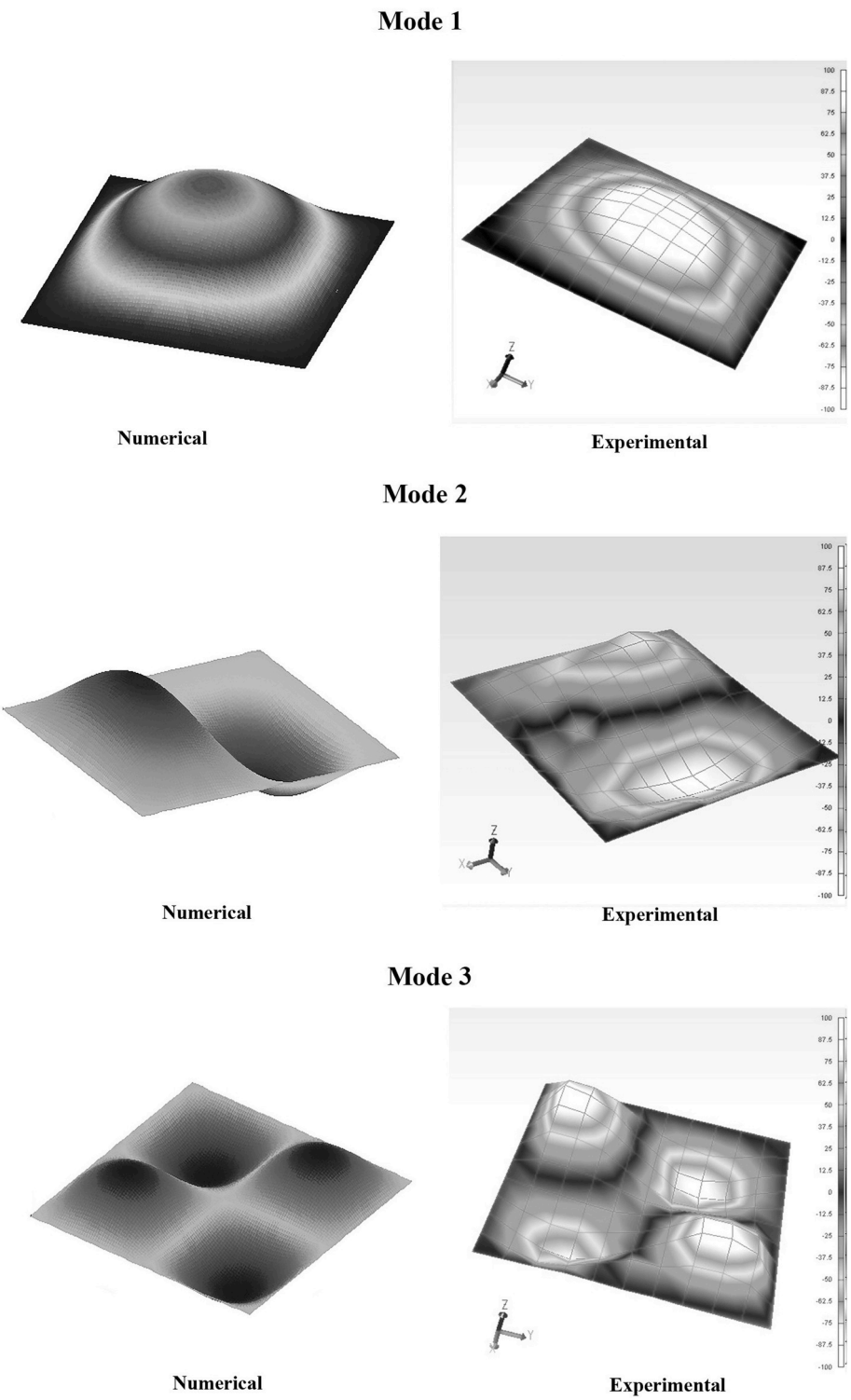

Fig. 6. Numerical and experimental mode shapes for lowest three modal frequencies at temperature rise of 100 °C.

Table 3
CrossMAC matrix for comparison of experimental and theoretical mode shapes.

Frequency (Hz)	Experimental		
Numerical	134.86	373.81	544.65
132.27	**0.9020**	0.5314	0.2385
366.16	0.5299	**0.9214**	0.7687
529.71	0.2150	0.7635	**0.9436**

specific time interval, the BMRP being at the higher side. The modal analysis is carried out for different moisture content to understand the free vibration behaviour of composite laminates in moist environment. The results in terms of natural frequencies obtained from the nonlinear FE model and experiments are compared for laminates with various boundary conditions. The natural frequencies obtained for free-free boundary condition are presented in Table 4 and the fundamental frequencies obtained for simply supported and clamped boundary conditions are presented in Fig. 8.

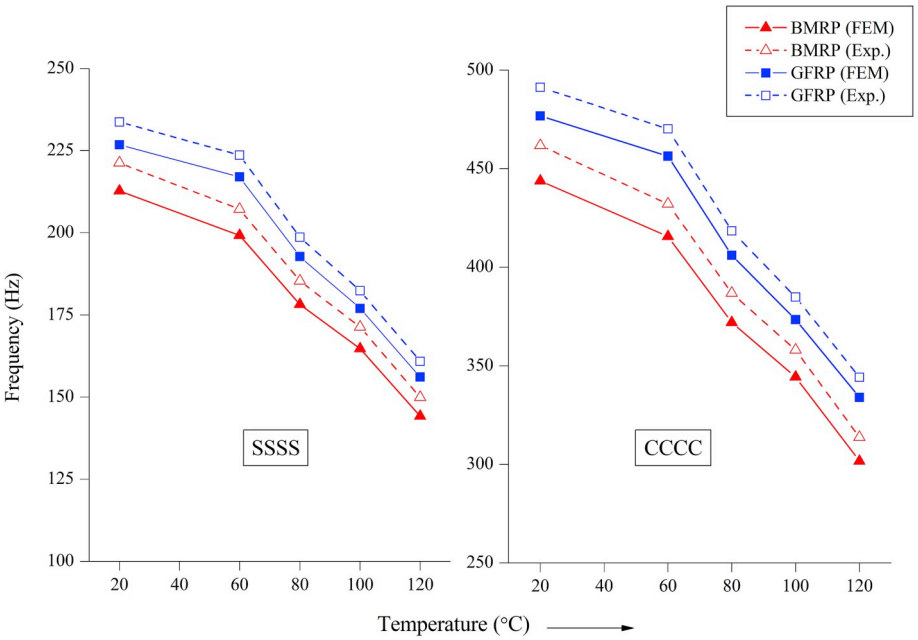

Fig. 7. Influence of temperature rise on the variation of fundamental frequencies of GFRP and BMRP laminates for simply supported (SSSS) and clamped (CCCC) boundary conditions.

It is observed from Table 4 that the natural frequencies get reduced significantly with increased moisture concentration for both GFRP and BMRP laminates in fully immersed condition. Similarly the reduction of natural frequencies with increment of moisture concentration for simply supported as well as clamped boundary condition is also evident from Fig. 8. The natural frequencies obtained from the present FE formulation and experiments are in good agreement. The percentage deviation between the natural frequencies calculated from the present FE model and experimental study remains below 5% irrespective of boundary conditions and moisture concentration. The reduction in natural frequencies is within the expected line because the stiffness of plate is reduced significantly due to the initial stresses induced by elevated moisture content. Moreover the moisture absorbed by the laminates increases mass of the laminates which in turn reduces the natural frequencies of the laminates. The percentage reduction of the natural frequency is calculated for the highest probable moisture absorption with respect to the natural frequencies obtained for dry laminates at ambient temperature. The frequencies of the first three modes of GFRP laminates reduce by 40.08%, 38.8% and 37.74% respectively for 1.75% moisture absorption. The percentage reduction of frequencies for BMRP laminates are found to be 60%, 57.36% and 52.64% respectively for first three modes at 1.9% moisture concentration. It is noted that the BMRP laminates are affected more in moist environment as an obvious reason resulting in more reduction in frequencies. This is because of using untreated bamboo sticks in BMRP laminates instead of bamboo fibres, which resulted in increased contact area with water at edges.

4.4. *Comparative study of GFRP and BMRP laminates*

A comparative study on the free vibration behaviour of GFRP and BMRP laminates under hygrothermal effect is carried out in order to check the efficiency of bamboo stick/fibre as a viable alternative of synthetic fibre. The laminates (a/b = 1 and a/t = 50) with simply supported boundary condition are considered for the study. The difference in the fundamental natural frequency, obtained from present FEM, for elevated temperature and moisture absorption is presented and compared in Table 5. The percentage reduction in the fundamental frequencies of GFRP and BMRP laminates under the combined effect of elevated temperature and moisture concentration are obtained and compared in Fig. 9.

It is observed from Table 5 that the average difference of the fundamental frequency between GFRP and BMRP laminate is 7.38% for different level of temperature increment, which is not very significant. On the other hand, the difference between the fundamental frequencies of GFRP and BMRP laminates for moisture absorption keeps increasing with increase in moisture content and reaches maximum of 20% at

Table 4
Natural frequencies for free-free GFRP and BMRP laminates at different moisture concentration.

Type of laminate	ΔC (%)	Natural frequencies (Hz)						Deviation (%)		
		FEM			Experimental			(Experimental-FEM)/Experimental		
		Mode 1	Mode 2	Mode 3	Mode 1	Mode 2	Mode 3	Mode 1	Mode 2	Mode 3
GFRP	0.7	181.93	501.44	727.41	185.78	511.74	744.23	2.07	2.01	2.26
	1.2	157.00	432.73	627.74	160.31	441.38	642.56	2.06	1.96	2.31
	1.6	137.00	377.61	547.79	139.99	385.12	560.38	2.14	1.95	2.25
	1.75	**114.15**	**321.35**	**474.24**	**116.60**	**327.66**	**485.30**	**2.10**	**1.93**	**2.28**
BMRP	1.5	124.33	349.91	505.31	127.46	357.49	518.17	2.46	2.12	2.48
	1.75	**102.28**	**287.91**	**421.63**	**104.88**	**294.11**	**432.43**	**2.48**	**2.11**	**2.50**
	1.8	98.39	275.39	401.89	100.86	281.40	411.91	2.45	2.14	2.43
	1.9	91.82	258.42	373.19	94.11	264.11	382.59	2.43	2.15	2.46
Difference (%) (GFRP-BMRP) at ΔC = 1.75%		10.40	10.41	11.09	10.05	10.24	10.89	–	–	–

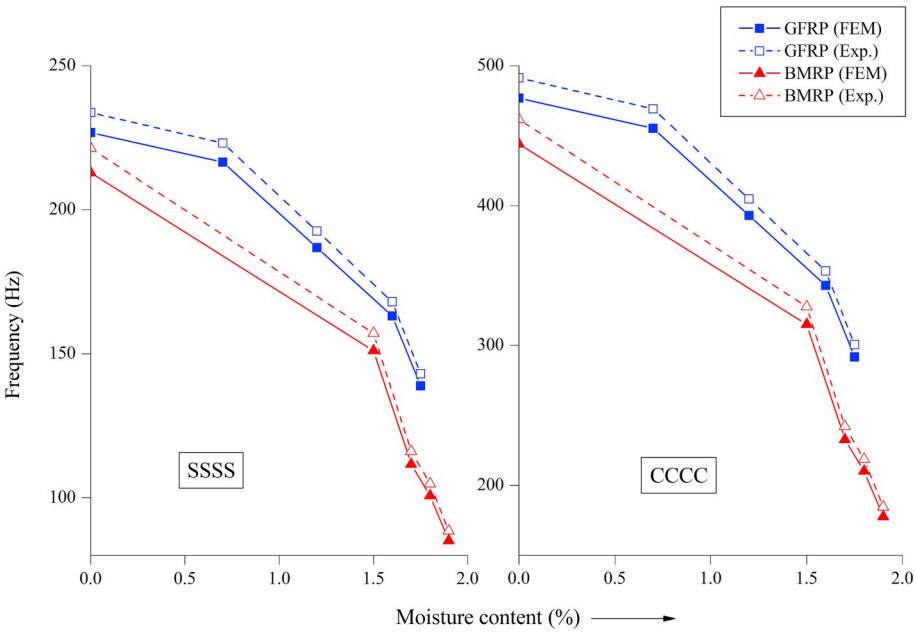

Fig. 8. Effect of moisture absorption on the variation of fundamental frequencies of GFRP and BMRP laminates for simply supported (SSSS) and clamped (CCCC) boundary conditions.

Table 5
Comparison between fundamental frequencies (in Hz) of GFRP and BMRP laminates for temperature rise (ΔT) and moisture absorption (ΔC).

Hygrothermal condition		GFRP	BMRP	% difference (GFRP-BMRP)/GFRP
ΔT	60 °C	192.80	178.20	7.57
	80 °C	177.00	164.76	6.92
	100 °C	156.07	144.15	7.64
ΔC	1.5	174.91	151.09	13.62
	1.6	163.1	138.62	15.01
	1.7	140.68	111.58	20.69

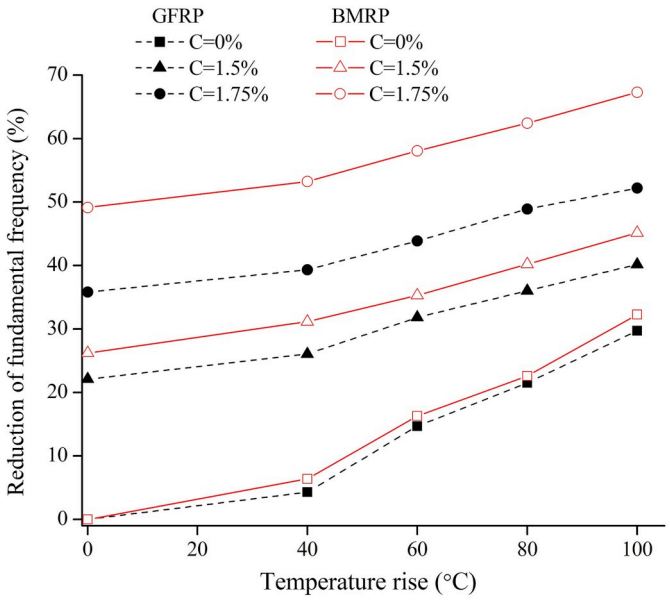

Fig. 9. Variation of fundamental frequencies between GFRP and BMRP laminates under hygrothermal effect.

saturation state. It is evident from Fig. 9 that the reduction of natural frequencies is higher for BMRP laminate than that of GFRP laminate under hygrothermal environment. It is also noted that the difference between reduction percentage of frequency of GFRP and BMRP is very less at dry condition. Even for lower moisture concentration the difference is not very significant. The variation becomes higher as the moisture concentration increases and the difference becomes significant in fully immersed condition.

5. Conclusion

Experimental and numerical studies on free vibration of GFRP and BMRP composite laminates are carried out with varying temperature rise, moisture absorption and combined hygrothermal condition. The elastic properties of GFRP and BMRP laminate decrease with the increase in temperature and moisture content which alter the natural frequencies consequently. Experiments are conducted for different levels of temperature rise and moisture absorption considering various support conditions including simply supported, clamped and free-free boundary condition. The inference drawn from the observations of the results are abridged as follows:

i The moisture absorption pattern in both GFRP and BMRP laminates follows Fickian type of diffusion. The amount of water uptake is higher when exposed to tap water compared to that in saline water due to higher density of saline water. The maximum amount of water uptake in GFRP and BMRP laminates is 1.75% and 1.9% respectively for same period of immersion in tap water in the most severe moisture absorption in fully immersed condition. Locally available untreated bamboo is the weakest form and absorbs moisture significantly.

ii The natural frequencies obtained from the experimental investigation as well as FE modelling show excellent agreement for all type of boundary conditions. The natural frequencies decrease with the increase in temperature and moisture concentration for both GFRP and BMRP laminates due to reduction in stiffness of laminates irrespective of boundary conditions.

iii The numerical values of MAC indicate excellent correlation and consistency between the mode shapes obtained numerically and experimentally.
iv The fundamental frequencies of GFRP and BMRP laminates increase linearly with the decreasing thickness ratio as the stiffness of laminates increase with the thicker laminates.

Based on the above observations, it is concluded that the dynamic behaviours of bamboo epoxy composites and glass epoxy composites under hygrothermal effect are of identical pattern. Therefore, bamboo epoxy laminates can be used as potential substitute of glass epoxy laminates in composite structures to achieve environment friendly and economic design where moisture exposure is low. However better performance of bamboo epoxy laminates in moist environment may be acquired by using chemically and physically treated bamboo fibres. The properties of bamboo fibre can be improved by proper treatment and drying process before fabricating the laminates.

Acknowledgements

This research did not receive any specific grant from funding agencies in the public, commercial, or not-for-profit sectors.

Appendix A

$$\begin{Bmatrix} \varepsilon_{xnl} \\ \varepsilon_{ynl} \\ \gamma_{xynl} \\ \gamma_{xznl} \\ \gamma_{yznl} \end{Bmatrix} = \begin{Bmatrix} \frac{1}{2}\left[\left(\frac{\partial U}{\partial x}\right)^2 + \left(\frac{\partial V}{\partial x}\right)^2 + \left(\frac{\partial W}{\partial x}\right)^2\right] \\ \frac{1}{2}\left[\left(\frac{\partial U}{\partial y}\right)^2 + \left(\frac{\partial V}{\partial y}\right)^2 + \left(\frac{\partial W}{\partial y}\right)^2\right] \\ \frac{\partial U}{\partial x}.\frac{\partial U}{\partial y} + \frac{\partial V}{\partial x}.\frac{\partial V}{\partial y} + \frac{\partial W}{\partial x}.\frac{\partial W}{\partial y} \\ \frac{\partial U}{\partial x}.\frac{\partial U}{\partial z} + \frac{\partial V}{\partial x}.\frac{\partial V}{\partial z} \\ \frac{\partial U}{\partial y}.\frac{\partial U}{\partial z} + \frac{\partial V}{\partial y}.\frac{\partial V}{\partial z} \end{Bmatrix} \tag{A.1}$$

$$\mathbf{B}_{NL} = \sum_{i=1}^{8} \begin{bmatrix} \partial S_i/\partial x & 0 & 0 & 0 & 0 & 0 & 0 \\ \partial S_i/\partial y & 0 & 0 & 0 & 0 & 0 & 0 \\ 0 & \partial S_i/\partial x & 0 & 0 & 0 & 0 & 0 \\ 0 & \partial S_i/\partial y & 0 & 0 & 0 & 0 & 0 \\ 0 & 0 & \partial S_i/\partial x & 0 & 0 & 0 & 0 \\ 0 & 0 & \partial S_i/\partial y & 0 & 0 & 0 & 0 \\ 0 & 0 & 0 & \partial S_i/\partial x & 0 & 0 & 0 \\ 0 & 0 & 0 & \partial S_i/\partial y & 0 & 0 & 0 \\ 0 & 0 & 0 & 0 & \partial S_i/\partial x & 0 & 0 \\ 0 & 0 & 0 & 0 & \partial S_i/\partial y & 0 & 0 \\ 0 & 0 & 0 & 0 & 0 & \partial S_i/\partial x & 0 \\ 0 & 0 & 0 & 0 & 0 & \partial S_i/\partial y & 0 \\ 0 & 0 & 0 & 0 & 0 & 0 & \partial S_i/\partial x \\ 0 & 0 & 0 & 0 & 0 & 0 & \partial S_i/\partial y \\ 0 & 0 & 0 & S_i & 0 & 0 & 0 \\ 0 & 0 & 0 & 0 & S_i & 0 & 0 \\ 0 & 0 & 0 & 0 & 0 & S_i & 0 \\ 0 & 0 & 0 & 0 & 0 & 0 & S_i \end{bmatrix} \tag{A.2}$$

$$\mathbf{L} = \begin{bmatrix} L_{11} & & & & & & & & & & & & & & & & & \\ L_{21} & L_{22} & & & & & & & & & & & & & & & & \\ 0 & 0 & L_{33} & & & & & & & & & & & & & & & \\ 0 & 0 & L_{43} & L_{44} & & & & & & & & & & & & & & \\ 0 & 0 & 0 & 0 & L_{55} & & & & & & & & & & & & & \\ 0 & 0 & 0 & 0 & L_{65} & L_{66} & & & & & & & & & & & & \\ L_{71} & L_{72} & 0 & 0 & 0 & 0 & L_{77} & & & & & & & & & & & \\ L_{81} & L_{82} & 0 & 0 & 0 & 0 & L_{87} & L_{88} & & & & & & & & & & \\ 0 & 0 & L_{93} & L_{94} & 0 & 0 & 0 & 0 & L_{99} & & & & & & & & & \\ 0 & 0 & L_{103} & L_{104} & 0 & 0 & 0 & 0 & L_{109} & L_{1010} & & & & & & & & \\ L_{111} & L_{112} & 0 & 0 & 0 & 0 & 0 & 0 & 0 & 0 & L_{1111} & & & & & & & \\ L_{121} & L_{122} & 0 & 0 & 0 & 0 & 0 & 0 & 0 & 0 & L_{1211} & L_{1212} & & & & & & \\ 0 & 0 & L_{133} & L_{134} & 0 & 0 & 0 & 0 & 0 & 0 & 0 & 0 & L_{1313} & & & & & \\ 0 & 0 & L_{143} & L_{144} & 0 & 0 & 0 & 0 & 0 & 0 & 0 & 0 & L_{1413} & L_{1414} & & & & \\ L_{151} & L_{152} & 0 & 0 & 0 & 0 & 0 & 0 & 0 & 0 & 0 & 0 & 0 & 0 & 0 & & & \\ 0 & 0 & L_{163} & L_{164} & 0 & 0 & 0 & 0 & 0 & 0 & 0 & 0 & 0 & 0 & 0 & 0 & & \\ L_{171} & L_{172} & 0 & 0 & 0 & 0 & 0 & 0 & 0 & 0 & 0 & 0 & 0 & 0 & 0 & 0 & 0 & \\ 0 & 0 & L_{183} & L_{184} & 0 & 0 & 0 & 0 & 0 & 0 & 0 & 0 & 0 & 0 & 0 & 0 & 0 & 0 \end{bmatrix} \tag{A.3}$$

Terms of **L** matrix

$L_{11} = L_{33} = L_{55} = N_x^i$; $L_{22} = L_{44} = L_{66} = N_y^i$; $L_{21} = L_{43} = L_{65} = N_{xy}^i$

$$L_{77} = L_{99} = N_x^i t^2 \Big/ 12 \;\; ; L_{88} = L_{1010} = N_y^i t^2 \Big/ 12 \;\; ; L_{87} = L_{109} = N_{xy}^i t^2 \Big/ 12$$

$$L_{71} = L_{93} = M_x^i; L_{82} = L_{104} = M_y^i; L_{72} = L_{81} = L_{94} = L_{103} = M_{xy}^i$$

$$L_{111} = L_{133} = P_x^i; L_{122} = L_{144} = P_y^i; L_{112} = L_{121} = L_{134} = L_{143} = P_{xy}^i$$

$$L_{1111} = L_{1313} = M_x^i t^2 \Big/ 12; L_{1212} = L_{1414} = M_y^i t^2 \Big/ 12; L_{1212} = L_{1413} = M_{xy}^i t^2 \Big/ 12$$

$$L_{151} = L_{163} = Q_x^i; L_{152} = L_{164} = Q_y^i; L_{171} = L_{183} = R_x^i; L_{172} = L_{184} = R_y^i$$

Appendix B

The MAC value between two modes is the normalized dot product of two sets of modal vectors $\{\Psi_N\}$ and $\{\Psi_E\}$. The resulting scalars are arranged into the MAC matrix:

$$MAC(\{\Psi_N\},\{\Psi_E\}) = \frac{\left|\{\Psi_N\}^T\{\Psi_E\}\right|^2}{(\{\Psi_N\}^T\{\Psi_N\})(\{\Psi_E\}^T\{\Psi_E\})} \quad \text{(B.1)}$$

$\{\Psi_N\}$ = Modal vector obtained from numerical analysis

$\{\Psi_E\}$ = Modal vector obtained from experiment

Appendix C. Supplementary data

Supplementary data to this article can be found online at https://doi.org/10.1016/j.compositesb.2019.107333.

References

[1] Huda S, Reddy N, Yang Y. Ultra-light-weight composites from bamboo strips and polypropylene web with exceptional flexural properties. Compos B 2012;43(3):1658–64.

[2] Manalo AC, Wani E, Zukarnain NA, Karunasena W, Lau K-T. Effects of alkali treatment and elevated temperature on the mechanical properties of bamboo fibre–polyester composites. Compos B 2015;80:73–83.

[3] Trujillo E, Moesen M, Osorio L, Vuure AV, Ivens J, Verpoest I. Bamboo fibres for reinforcement in composite materials: strength Weibull analysis. Compos A 2014;61:115–25.

[4] Amada S, Ichikawa Y, Munekata T, Nagase Y, Shimizu H. Fiber texture and mechanical graded structure of bamboo. Compos B 1997;28(1–2):13–20.

[5] Kabir M, Wang H, Lau K, Cardona F. Chemical treatments on plant-based natural fibre reinforced polymer composites: an overview. Compos B 2012;43(7):2883–92.

[6] Sukmawan R, Takagi H, Nakagaito AN. Strength evaluation of cross-ply green composite laminates reinforced by bamboo fiber. Compos B 2016;84:9–16.

[7] Yu Y, Huang X, Yu W. A novel process to improve yield and mechanical performance of bamboo fiber reinforced composite via mechanical treatments. Compos B 2014;56:48–53.

[8] Essabir H, Raji M, Laaziz SA, Rodrique D, Bouhfid R, Qaiss AEK. Thermo-mechanical performances of polypropylene biocomposites based on untreated, treated and compatibilized spent coffee grounds. Compos B 2018;149:1–11.

[9] Lee S-H, Wang S. Biodegradable polymers/bamboo fiber biocomposite with bio-based coupling agent. Compos A 2006;37(1):80–91.

[10] Li H-T, Su J-W, Zhang Q-S, Deeks AJ, Hui D. Mechanical performance of laminated bamboo column under axial compression. Compos B 2015;79:374–82.

[11] Kumar N, Mireja S, Khandelwal V, Arun B, Manik G. Light-weight high-strength hollow glass microspheres and bamboo fiber based hybrid polypropylene composite: a strength analysis and morphological study. Compos B 2017;109:277–85.

[12] Okubo K, Fujii T, Yamamoto Y. Development of bamboo-based polymer composites and their mechanical properties. Compos A 2004;35(3):377–83.

[13] Lu T, Liu S, Jiang M, Xu X, Wang Y, Wang Z, et al. Effects of modifications of bamboo cellulose fibers on the improved mechanical properties of cellulose reinforced poly(lactic acid) composites. Compos B 2014;62:191–7.

[14] Sujito Takagi H. Flexural strength and impact energy of microfibril bamboo fiber reinforced environment-friendly composites based on poly-lactic acid resin. Int J Mod Phys B 2011;25(31):4195–8.

[15] Tokoro R, Vu DM, Okubo K, Tanaka T, Fujii T, Fujiura T. How to improve mechanical properties of polylactic acid with bamboo fibers. J Mater Sci 2007;43(2):775–87.

[16] Takagi H, Kako S, Kusano K, Ousaka A. Thermal conductivity of PLA-bamboo fiber composites. Adv Compos Mater 2007;16(4):377–84.

[17] Khan Z, Yousif B, Islam M. Fracture behaviour of bamboo fiber reinforced epoxy composites. Compos B 2017;116:186–99.

[18] Fu Y, Fang H, Dai F. Study on the properties of the recombinant bamboo by finite element method. Compos B 2017;115:151–9.

[19] Thwe MM, Liao K. Effects of environmental aging on the mechanical properties of bamboo–glass fiber reinforced polymer matrix hybrid composites. Compos A 2002;33(1):43–52.

[20] Jain S, Kumar R, Jindal UC. Mechanical behaviour of bamboo and bamboo composite. J Mater Sci 1992;27(17):4598–604.

[21] Jindal U. Development and testing of bamboo-fibres reinforced plastic composites. J Compos Mater 1986;20(1):19–29.

[22] Verma C, Chariar V. Development of layered laminate bamboo composite and their mechanical properties. Compos B 2012;43(3):1063–9.

[23] Verma C, Chariar V. Stiffness and strength analysis of four layered laminate bamboo composite at macroscopic scale. Compos B 2013;45(1):369–76.

[24] Li H-T, Zhang Q-S, Huang D-S, Deeks AJ. Compressive performance of laminated bamboo. Compos B 2013;54:319–28.

[25] Chen H, Miao M, Ding X. Influence of moisture absorption on the interfacial strength of bamboo/vinyl ester composites. Compos A 2009;40(12):2013–9.

[26] Samal SK, Mohanty S, Nayak SK. Polypropylene—bamboo/glass fiber hybrid composites: fabrication and analysis of mechanical, morphological, thermal, and dynamic mechanical behaviour. J Reinf Plast Compos 2008;28(22):2729–47.

[27] Qian S, Zhang H, Yao W, Sheng K. Effects of bamboo cellulose nanowhisker content on the morphology, crystallization, mechanical, and thermal properties of PLA matrix biocomposites. Compos B 2018;133:203–9.

[28] Thwe MM, Liao K. Environmental effects on bamboo-glass/polypropylene hybrid composites. J Mater Sci 2003;38(2):363–76.

[29] Godbole VS, Lakkad SC. Effect of water absorption on the mechanical properties of bamboo. J Mater Sci Lett 1986;5(3):303–4.

[30] Zakikhani P, Zahari R, Sultan M, Majid D. Extraction and preparation of bamboo fibre-reinforced composites. Mater Des 2014;63:820–8.

[31] Sit M, Ray C, Biswas D, Mandal B. Stress distribution in the hollow stiffened hybrid laminated composite panels in ship structures under sinusoidal loading. Int J Marit Eng 2016;158(A2):107–16.

[32] Biswas D, Ray C. Comparative perspective of various shear deformation theories with experimental verification for modal analysis of hybrid laminates. J Vib Control 2015;23(8):1321–33.

[33] Parameswaran N, Liese W. On the fine structure of bamboo fibres. Wood Sci Technol 1976;10(4):231–46.

[34] ASTM E494. 2010: Standard Practice for measuring ultrasonic velocity in materials. 2010.